

A CONTRIBUTION TO THE DESIGN OF HYDRAULIC LUBE PUMPS

Salvatore Mancò, Nicola Nervegna and Massimo Rundo

The Fluid Power Research Laboratory at Polytechnic of Turin Politecnico di Torino, Corso Duca degli Abruzzi 24, 10129 Torino, Italia
niner@polito.it

Abstract

With special reference to gerotor lube pumps the paper details how a simulation environment can be instrumental in design development. The relevance of testing is stressed as an essential counterpart to simulation. Original modelling techniques are also proposed that provide a unified approach to volumetric pumps studies.

keywords: gerotor pumps, design, simulation and testing in fluid power

1 Introduction

At the Fluid Power Research Laboratory, experience with the AMESim™ simulation environment started in 1994 and has covered the simulation of various hydraulic components, i.e., pumps (internal and external gear, vane, axial and radial piston units), valves (pressure relief, counterbalance, flow force compensated spools, flow amplifiers), automotive control in hydrostatic transmissions, anti-lock braking systems (ABS), variable valve actuation (VVA) and systems. However, the present paper will focus on gerotor pumps. These are widely used in IC engines lubrication systems at low operating pressures but are also envisaged as substitutes to external gear pumps in high pressure automotive applications as they qualify as more gentle fluid-borne noise sources than external gear units. It is the scope of this paper to show how a simulation environment can be a valuable help in the course of a design process of a virtual gerotor unit that has to fulfill specific and stringent requirements.

However, attainment of this far reaching scope rests on two essential paradigms:

- It is impossible to develop an effective and faithful simulation of a hydraulic component unless it is investigated and known as intimately as possible.
- Simulation and testing must be strongly intertwined if predictive analyses of virtual prototypes will be exploited.

2 The Hydraulic Component

Basically, the unit consists of a pair of gear shaped elements mated so that each tooth of the inner gear is always in sliding contact with the outer gear to form sealed pockets of fluid. Both gears rotate in the same direction at low relative speeds with the inner gear being slightly faster. Fluid enters the chamber with increasing volume, is trapped in the spaces between the teeth and is transported to the outlet (Mancò, 1998). The gearing portion of the gerotor pump is shown in Fig. 1 whereas Fig. 2 shows the complete unit.

A basic circuit schematic is presented in Fig. 3. Oil is taken in from the tank (oil sump), passes through the inlet duct and is filtered (strainer). Delivered flow is further filtered and, pending on pressure level, excess flow is recirculated to inlet through a pressure relief valve. Downstream, the delivery duct port P is connected to lubricating oil consumers (load).

3 The Problems to be Solved

Dealing with a shaft mounted pump unit, two problems emerge at high engine speed (Mancò, 1999):

- excess flow must be recirculated (Mancò, 2001),
- airborne noise is strongly emphasized (Mancò, 2000).

Recirculation of excess flow postulates the intervention of the pressure relief valve and this entails power dissipation. The question: is there a way of achieving energy savings through a drastic removal of this valve?

This manuscript was received on 26 June 2001 and was accepted after revision for publication on 5 April 2002

As to the second problem the question is twofold. What is causing the excessive noise? And is there a remedy?

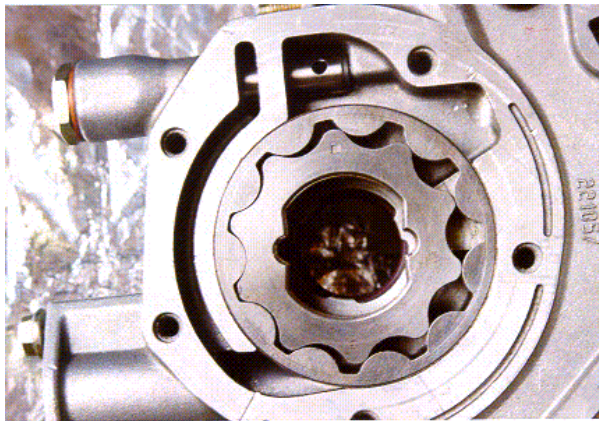


Fig. 1: Pump gearing and relief valve

4 The Stepped Approach to Simulation

If simulation is the tool to tackle the above problems the first paradigm comes into effect. This is to say that the core portion of the pump i.e. its gearing must be studied thoroughly (Fabiani, 1999; Mancò G, 2000). This is not an easy task and requires a patient and rigorous insight into gear profiles generation. At that level, one has to determine the line of contact of the engaging gears. Moreover, reminding a basic equation in volumetric pump studies:

$$\frac{dp_j}{dt} = \frac{\beta}{V_j} \left(Q_{in,j} - Q_{out,j} - \omega \frac{dV_j}{d\phi} \right) \quad j=1, 2, \dots, N \quad (1)$$

one has to acquire, for each variable volume chamber between the mating gears, quantitative knowledge about:

- volumes and volumes variations,
- inflow and outflow passage areas,
- working fluid bulk modulus.

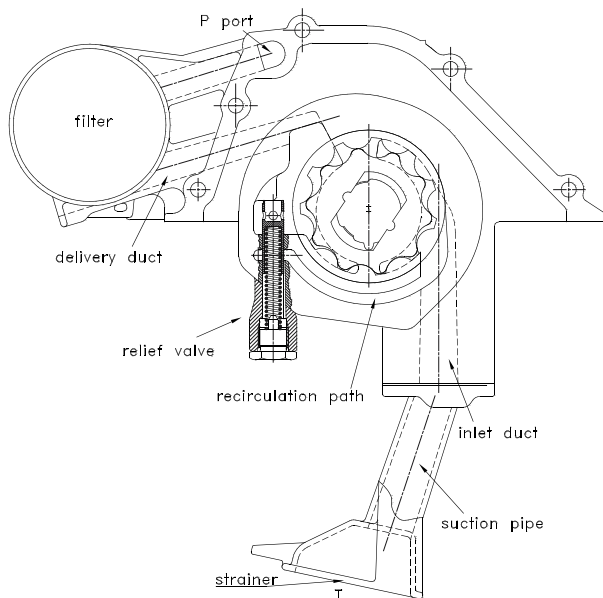


Fig. 2: Schematic layout of a complete unit

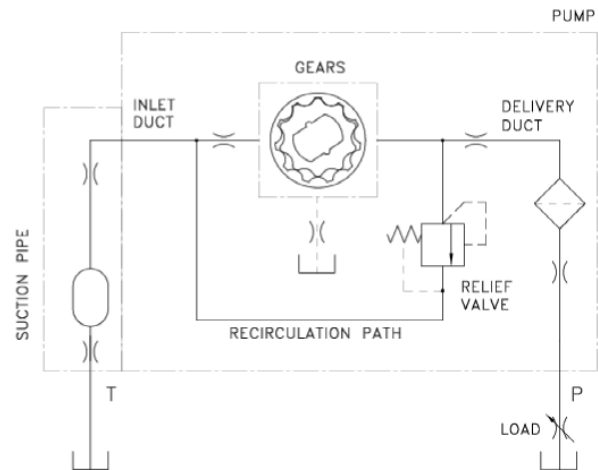


Fig. 3: Hydraulic circuit schematic

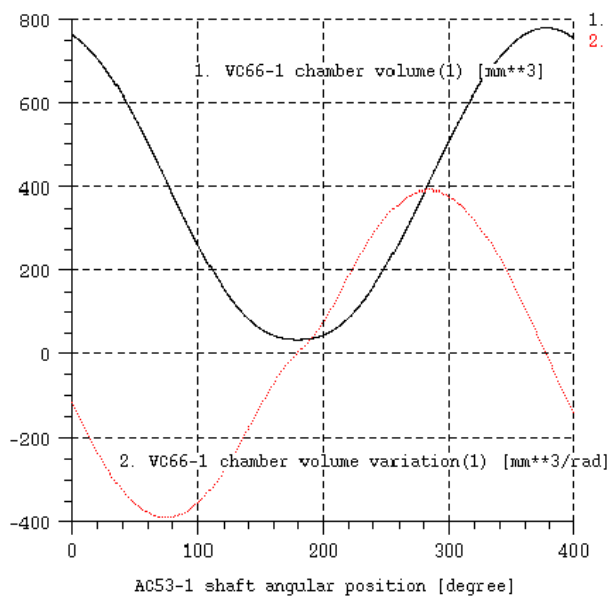


Fig. 4: Volume and volume variation

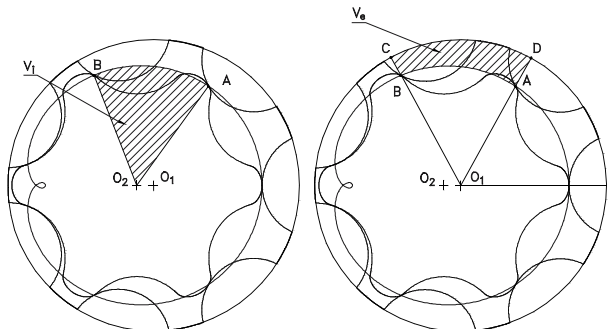


Fig. 5: Vector rays approach

As a first step one can assess an equivalent circuit schematic (see Fig. 3) where all the important items are already present, yet, before going any further the above aspects must be solved. Determination of volumes and volume variations can proceed from two different outlooks that, though yielding identical results, are very differently rated as far as computational time is concerned. The derivative-integral approach grounded on vector rays leads to a complete plot of chamber

and of its derivative (in a whole revolution of the external gear) in about 0.16 seconds (Fig. 4). Fig. 5 shows the basic concept of vector rays. The alternate approach (integral-derivative), that obtains volumes by integration of equations describing gear profiles and through numerical differentiation yields their derivatives, is about 600 times slower (Fabiani, 1999). The advantage of vector rays is that this same method can be put to fruition also for the determination of inflow and outflow passage areas between gearing and porting plate in both restricted and unrestricted geometries (see Fig. 6). This procedure has been implemented within the AMESim™ environment and yields results presented in Fig. 7.

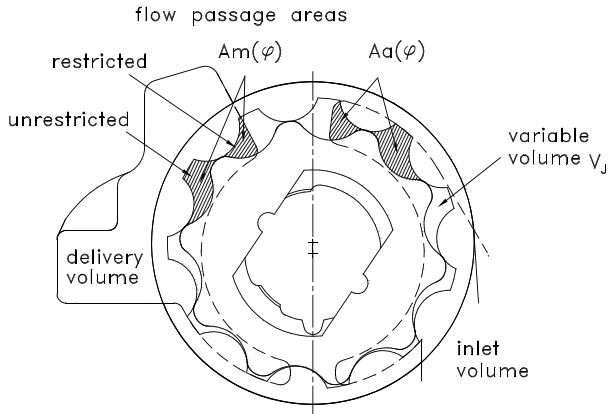


Fig. 6: Flow passage areas, restricted and unrestricted

The second step is bounded by the consideration that it is wise to start by following a modular approach. This means that since, in general, a volumetric pump possesses N variable chambers, there is no objection whatsoever in concentrating on the simplest possible one, that is, a unit with a single variable volume chamber. The clear cut advantage is that, by doing this, one is really laying down the foundations to simulate any type of volumetric pump whether it be external or internal gear, axial or radial piston, balanced or unbalanced vane. The module that must be considered is shown in Fig. 8 where crossport and external leakage paths are also accounted.

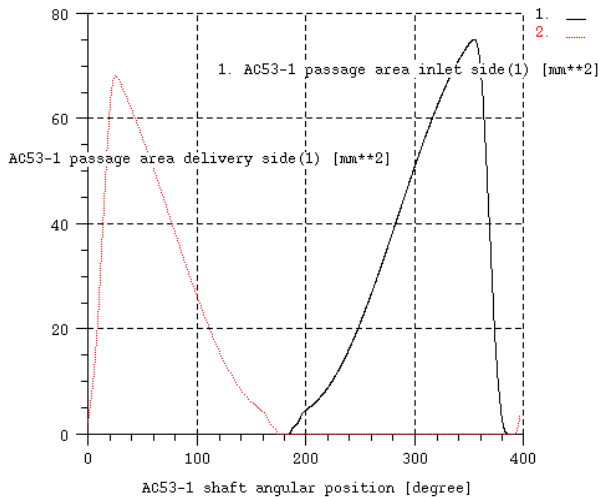


Fig. 7: Flow passage areas

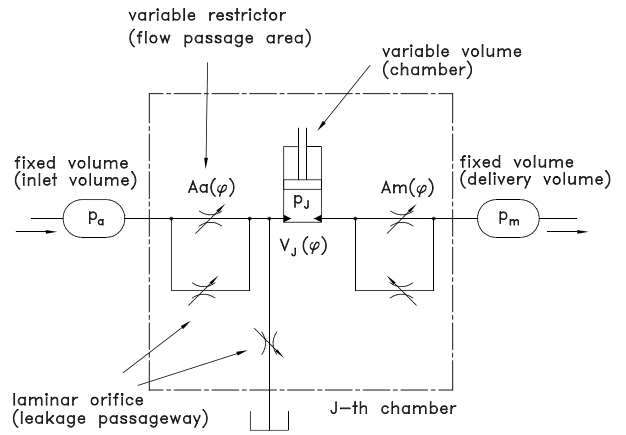


Fig. 8: Single variable volume chamber model

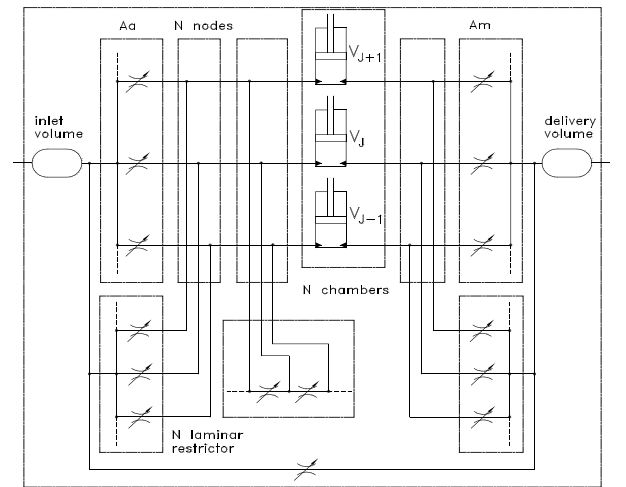


Fig. 9: N modular assemblies in parallel

The third step appears as a straightforward one. As many modules must be assembled in parallel as determined by the number of variable volume chambers of the pump. This leads to what is illustrated in Fig. 9. Yet this solution can become rather inconvenient the higher is the number of variable volume chambers. There is a strong need for synthesis and a very effective way to overcome this point has been devised: this is consequent to the conception of basic vector elements. The essential merit rests on the fact that the number N of variable volume chambers in the pump takes the role of an independent variable (a parameter in the AMESim™ context) fixed at will without significant interventions on the circuit. Vector submodels can be sorted into the following two categories: hydraulic and geometric. The first collects entities similar to AMESim™ standard submodels with the significant difference that input and output variables are vectors rather than scalars. To this category belong variable volumes, flow areas, nodes and hydraulic vector lines that are so conceived to be applicable to all types of volumetric pumps. An example in this category is presented in Fig. 10.

The dimension of each linear array vector is preset at 13 elements. Thus, the maximum number of variable volume chambers is $N_{max} = 13$. If $N < N_{max}$ vector elements with indices $(N+1)$ to N_{max} are empty.

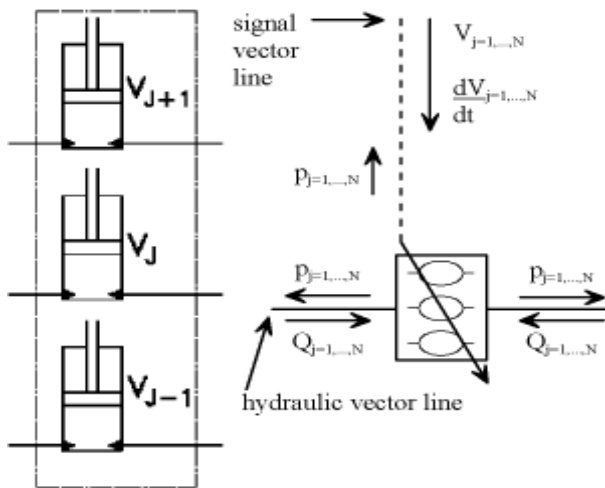


Fig. 10: Variable volume vector icon

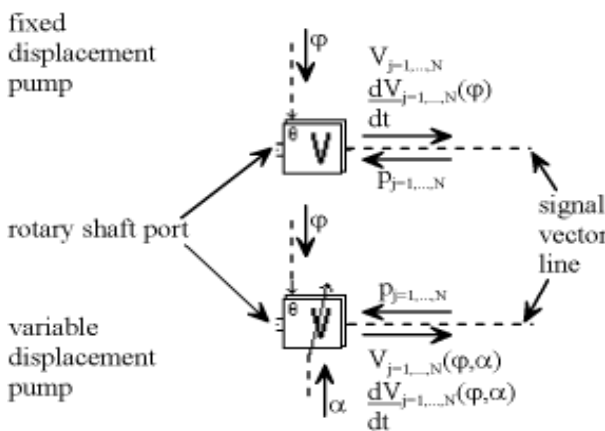


Fig. 11: Geometric vector icons for volumes and volumes derivatives in fixed and variable displacement pumps

Geometric submodels are, on their own, instrumental in providing appropriate informations (volumes, volumes derivatives, flow passage areas, etc) to the hydraulic submodels. In particular, geometric submodels can be *specific* to a given type of pump (e.g. gerotor, axial pistons, vane, etc.) or *general*. In the first case they already embody equations describing the geometry features of the pump under study in dependence of all intervening parameters (number of chambers, piston diameter, rotor thickness, etc.). In the second case data interpolation is effected on an input data file, otherwise, use can be made, as parameters, of equations devised by the user. Development of *specific* submodels requires from skilled users (the AMESet™ utility) and tuning time, however, parameters assignment and simulations are facilitated and gain large flexibility.

Adoption of *general* submodels does not involve the writing of a single line of code but introduces constraints in the simulation stage: if, for instance, geometry is provided as an input file, this has to be regenerated each time a change on a parameter has to be effected. Moreover, wishing to use a text parameter to input an equation (e.g. chamber volume as a function of shaft angle of rotation), its formulation has to be necessarily

simple.

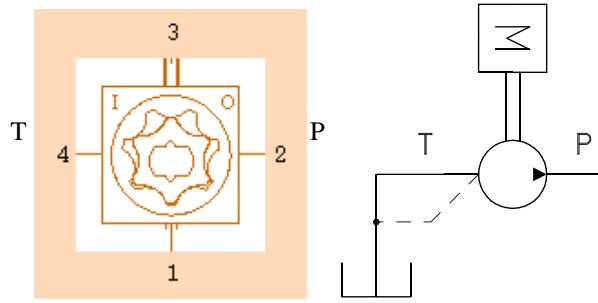


Fig. 12: The gerotor pump supercomponent

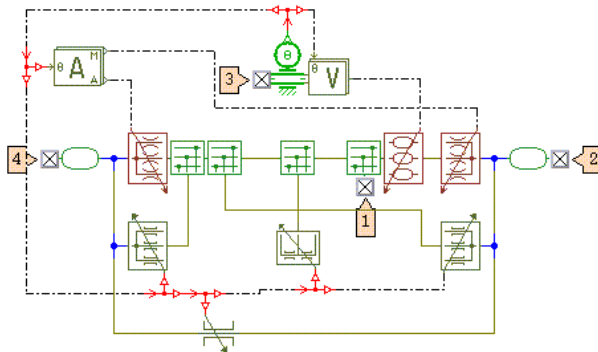


Fig. 13: Supercomponent details

A distinction must be made between fixed and variable displacement pumps. In the former, geometric data are only dependent on shaft angular position (gathered from an appropriate transducer), whereas in the latter, a dependence also exists on the displacement modulation factor (externally yielded by appropriate control strategies). Figure 11 shows geometric vector submodels icons for fixed and variable displacement pumps. Each icon must be associated with an appropriate submodel that typifies the specific pump (gear, vane, piston). For gerotor units, as shown earlier in this paper, the submodel is precisely grounded on the vector rays approach (Fig. 5) leading to plots illustrated in Fig. 4. An additional and expedient point for synthesis is already available within AMESim™ ^{super} and this is the *component*. Altogether this steers to the gerotor pump supercomponent depicted in Fig. 12. Figure 13 unveils what lays behind the curtains of the supercomponent icon.

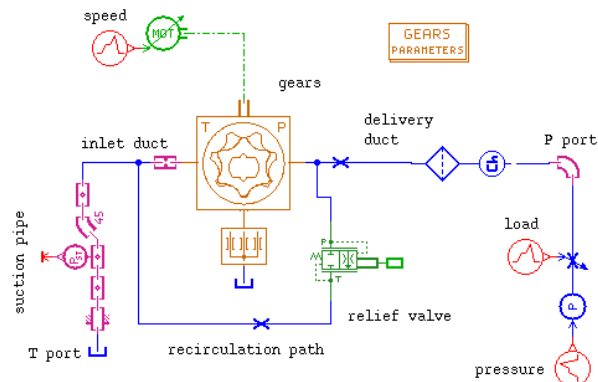


Fig. 14: The AMESim™

system for simulation

The *fourth step* finally leads to the AMESim™ system for simulation proposed in Fig. 14 where not only the gearing but also the relief valve are “iconised” as supercomponents.

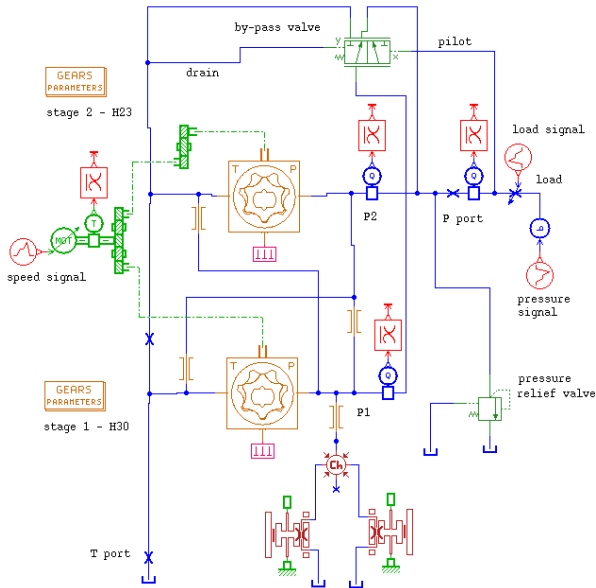


Fig. 15: Bi-rotor pump (18 chambers)

The advantage lies in the fact that these supercom-

ponents are readily reusable in the sense that it becomes relatively easy through these major “bricks” to assess more complex units such as the bi-rotor pump depicted in Fig. 15 or the variable displacement axial piston pump illustrated in Fig. 16.

In this last respect, Fig. 17 shows the details lumped into the supercomponent.

Handling of geometric data is global in that all informations that uniquely define the pump are collected into a submodel once and for all. This global submodel, through AMESim™ exports all data that can be then partaken by all submodels that need such informations. This procedure offers clear cut advantages. On one hand prevents the

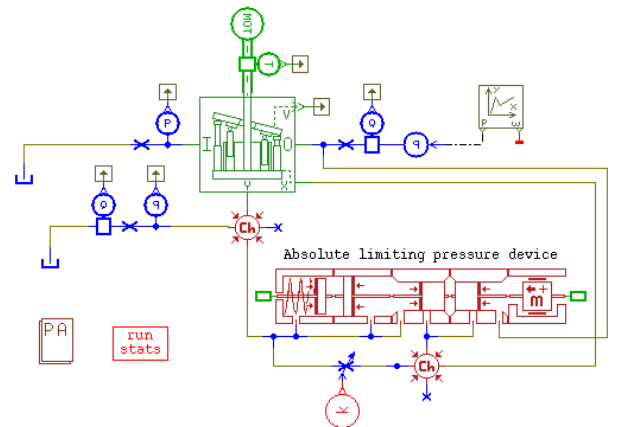


Fig. 16: Variable displacement axial piston pump

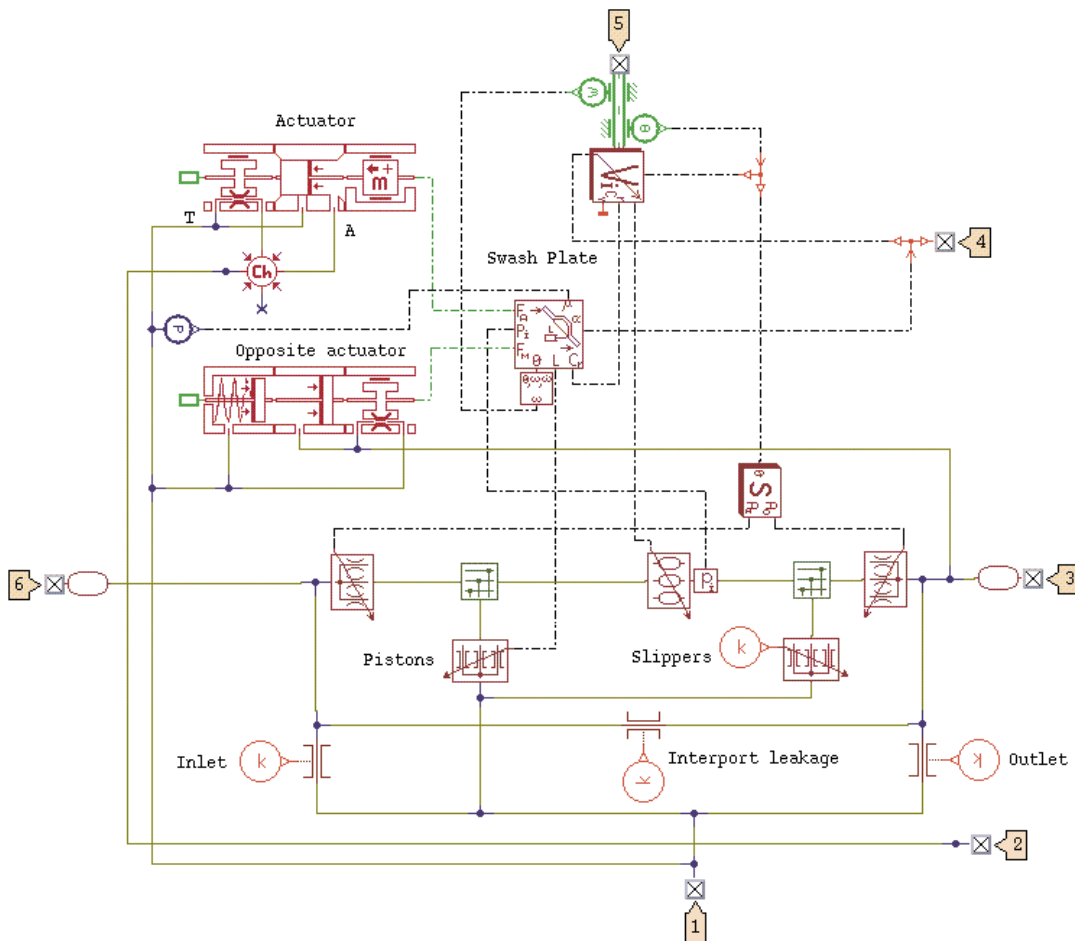
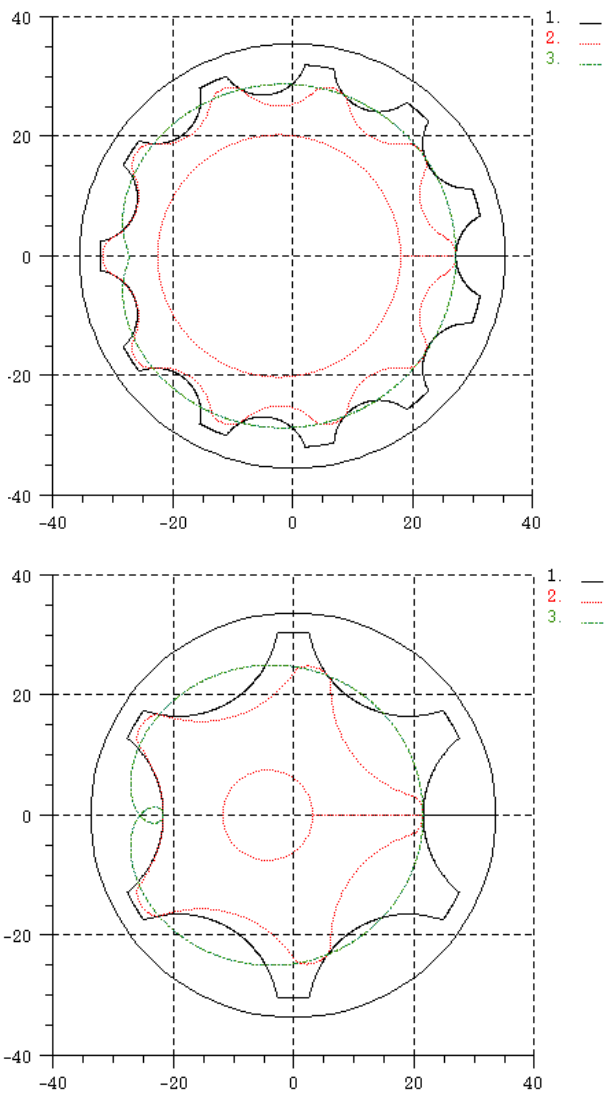


Fig. 17: *The unveiled supercomponent of the variable displacement axial piston pump*

annoying and time consuming effort of manually providing repeated and identical informations to whichever submodel (within a supercomponent) is in need of them, on the other hand is an objective safeguard against the chance of forgetting inputs to implied quests on the part of submodels and finally is a most convenient way of assessing a data base where a repository is organized to describe all geometric features of pump units belonging to a specific family.

Appendix A provides further considerations as to advantages stemming from the use of vector rather than scalar submodels. Appendix B elaborates on the use of the Hydraulic Resistance Library when modelling the suction piping of a lube pump.

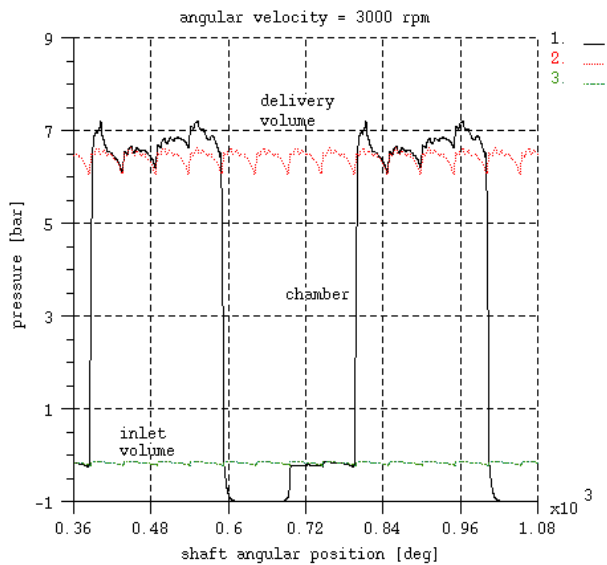
**Fig. 18:** *Mating gears profiles and lines of contacts*

5 Outcomes from Simulation Studies

Based on the steps outlined in the foregoing a significant number of quantitative and pertinent information can be gathered from simulation studies. These,

among others, can be specified as follows:

- determination of gears parameters subject to space limit constraints;
- drawing of the mating gears profiles and of their line of contacts (see Fig. 18);
- relative slip velocities;
- chamber volume and its derivative as functions of shaft angular position;
- chamber inflow and outflow passage areas;
- kinematic (ideal) flow ripple;
- steady state characteristics (flow vs. delivery pressure and flow vs. engine speed);
- real flow ripple;
- instantaneous chamber pressure time history (optimal timing analysis);
- instantaneous absorbed torque;
- flow losses (influence of geometry of leakage passageways).

**Fig. 19:** *Instantaneous pressure in delivery volume, inlet volume and variable volume chamber @ 3000 rpm*

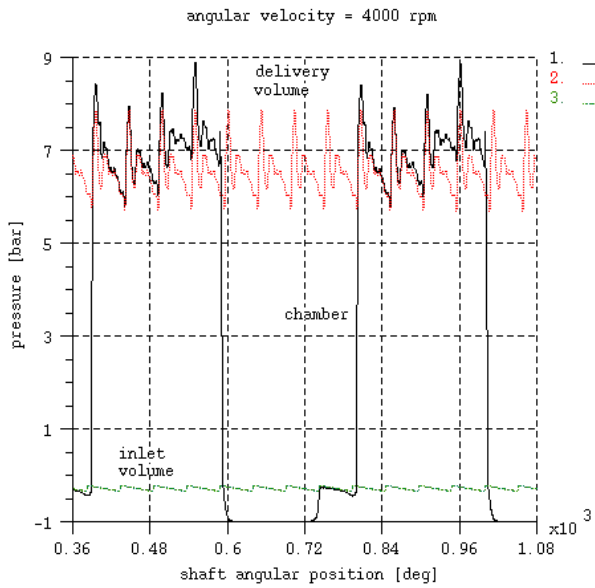


Fig. 20: Instantaneous pressure in delivery volume, inlet volume and variable volume chamber @4000 rpm

Examples of AMESim™ plots relative to the instantaneous pressure in a chamber, in the inlet and outlet volumes as functions of shaft angular position are shown for two angular velocity values in Fig. 19 and Fig. 20. Figure 21 shows the kinematic flow ripple yielded by units possessing even and odd variable volume chambers. Figure 22 shows instead the real flow ripple of each stage and the total flow rate of a bi-rotor pump.

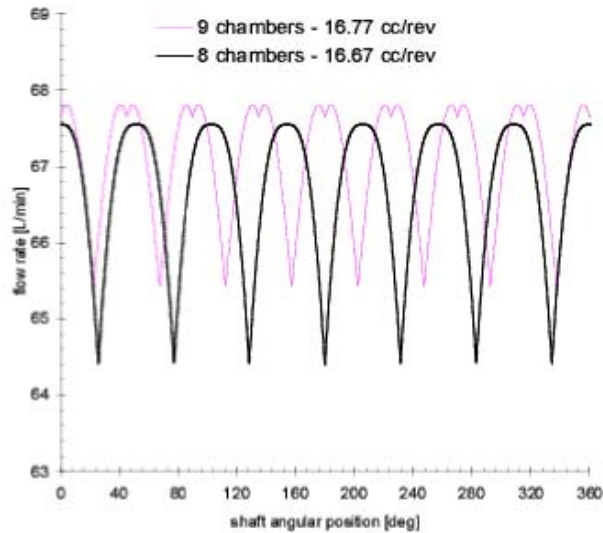


Fig. 21: Kinematic flow ripple (8 and 9 chambers)

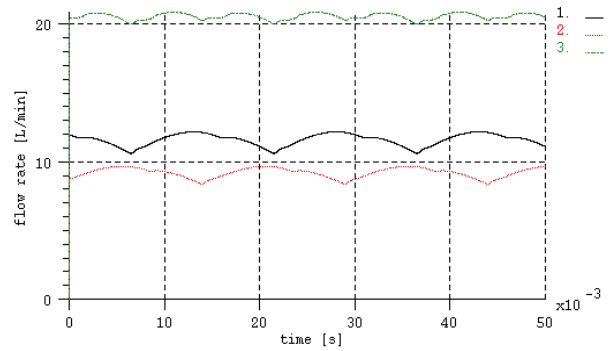


Fig. 22: Real flow ripple (bi-rotor pump with rotors phase shift of half pitch angle)

6 A Companion to Simulation

The second paradigm stresses the importance of testing during the progress of simulation studies. In this respect Fig. 23 shows a view of the rig for laboratory experiments. It is not only a problem of synergy between these two methodologies but also a permanent conviction and reaffirmation of the priority that testing must have on simulation. Both are precious arts and both require utmost care and rigor. It is on grounds of testing outcomes that we judge how good or bad our modelling is and how well it is progressing in portraying the real behaviour of the component under study. There are however physical facts that we are unable to simulate just because we are still far from grasping all

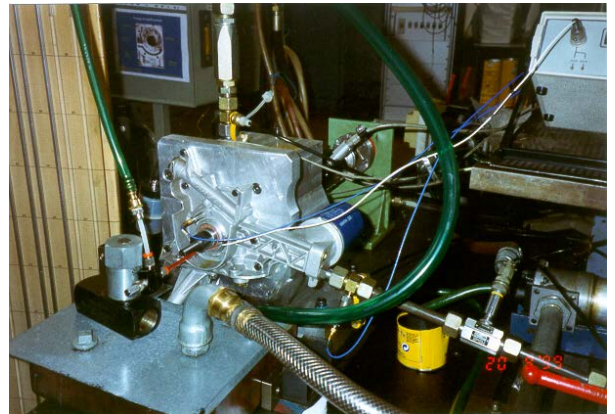


Fig. 23: A view of the experimental rig

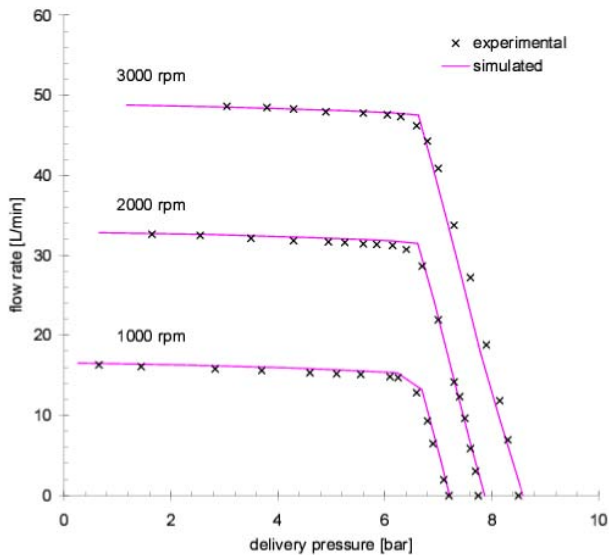


Fig. 24: Steady state characteristic (flow -pressure) as active. In fact a possibility exists of conceiving novel

their involved contents. It is on this side that simulation suffers its evident weaknesses and needs cooperative support from testing. Based on these thoughts Fig. 24 shows a comparison of experimental and simulated results of the steady state characteristic (flow-pressure) of the pump under study. It can be appreciated that the modelling and ensuing simulation is quite adequate in describing the truth as testified by testing. However, at high engine speed diversities come to evidence (see Fig. 25). Looking at Fig. 25, that shows experimental and simulated flow-speed steady state characteristic, at high speed a deviation of simulated results compared to experimental outcomes is apparent. If oil saturation pressure and the fractional content of separated air are both deemed constant irrespective of pump speed, then the experimental trend cannot be portrayed by simulation. To reproduce this factual behaviour it is necessary that either the saturation pressure or the fractional content of separated air be made dependent on engine speed. It is nonetheless unfortunate that even modest variations in such quantities lead to significant changes in flow rate. In this situation, demonstrated by experiments, simulation predicts wrong results just because what happens in reality is not known and being unknown is not part of the informative content fed into the modelling and therefore into the simulation. A long process involving thoughts and afterthoughts was needed prior to the understanding that incomplete (defective) chamber filling was the main cause for observed discrepancies. This was firmly proved by dedicated experiments and an elementary exercise in simulation by boosting the pump confirmed that the cause was identified (Mancò, 2001). Having identified the cause did not help much the simulation. In fact, based on our present knowledge and understanding, at high pump speed, it is not feasible to make a quantitative “a priori” prediction of the extent of the defective filling of pump chambers. Moreover, additional experimental outcomes highlighted, at high speed, the onset of intense pressure peaks (in the order of 10 bar) responsible in turn of

intolerable fluidborne noise (see Fig. 26). The diagnosis was rather easy: owing to incomplete filling at high speed, the connection with delivery originates an intense reverse flow into the chamber. An expansion wave propagates, followed, at complete filling, by a pressure peak.

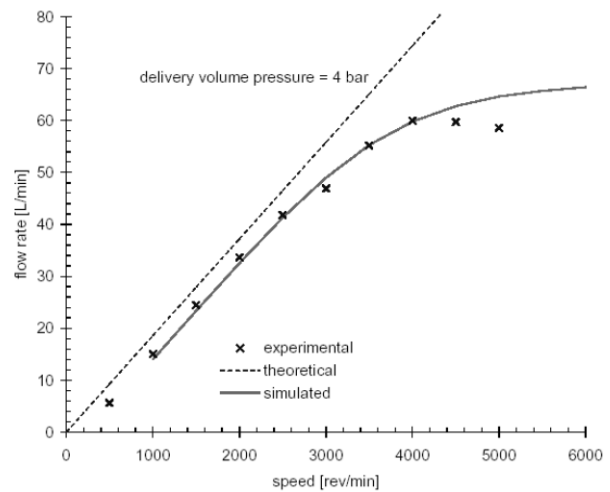


Fig. 25: Steady state characteristic (flow -speed)

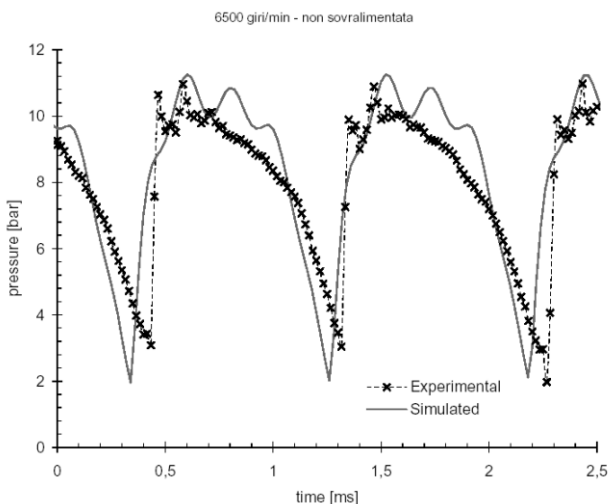


Fig. 26: Experimental and simulated delivery pressure @ 5000 rpm

7 A Search for Remedies

Some rather weak points emerge in this context regarding the modelling and simulation of fluid aeration and its impact on oil bulk modulus. The need is then apparent of gaining better insight into these phenomena so to improve the predictive capability of the AMESim™ environment. Yet other aspects also materialize related to possible remedial actions to the onset of excessive fluidborne noise. In this last respect at least three possibilities are envisaged. Two are to a certain extent passive and imply actions on (1) the geometry of silencing grooves to smooth reverse flow or (2) on port timing to dampen the pressure peaks. The third may be

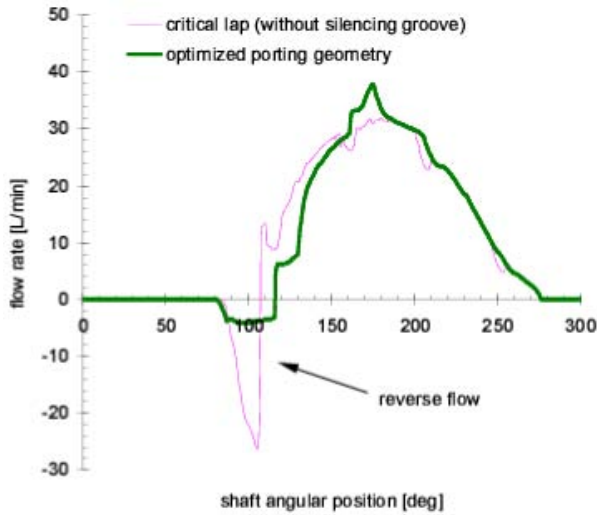


Fig. 27: A simulated comparison (optimal timing and silencing groove vs. ideal timing)

regarded gears to alleviate the problem (Mancò, 2000). It is towards the first two actions that AMESim™

thus limits the number of prototypes to be developed. So virtual units can be simulated looking at optimal port timing to diminish fluidborne noise (Mancò, 2000) or even variable timing units to match oil consumers' request and limit energy consumption (removal of the pressure relief valve) (Mancò, 2001). In this line of reasoning Fig. 27, arrived at through simulations, compares instantaneous flow rate generated by one out of N variable volume chambers of a virtual pump with ideal timing (critical lap and absence of silencing groove) against a solution where optimal timing and silencing groove have been embodied in the model. It can be appreciated that such a result does certainly provide significant insight and suggestions for design interventions.

8 Appendix A

An AMESim™ sketch that simulates a generic pump where the number of chambers can be varied at will ($N \leq N_{max}$) is shown in Fig. 28.

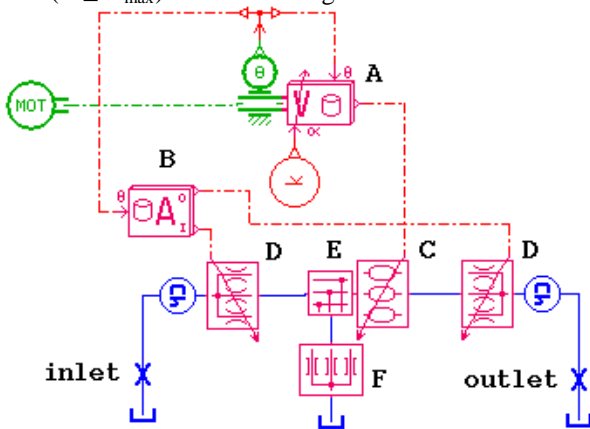


Fig. 28: A generic pump unit modelled with vector elements

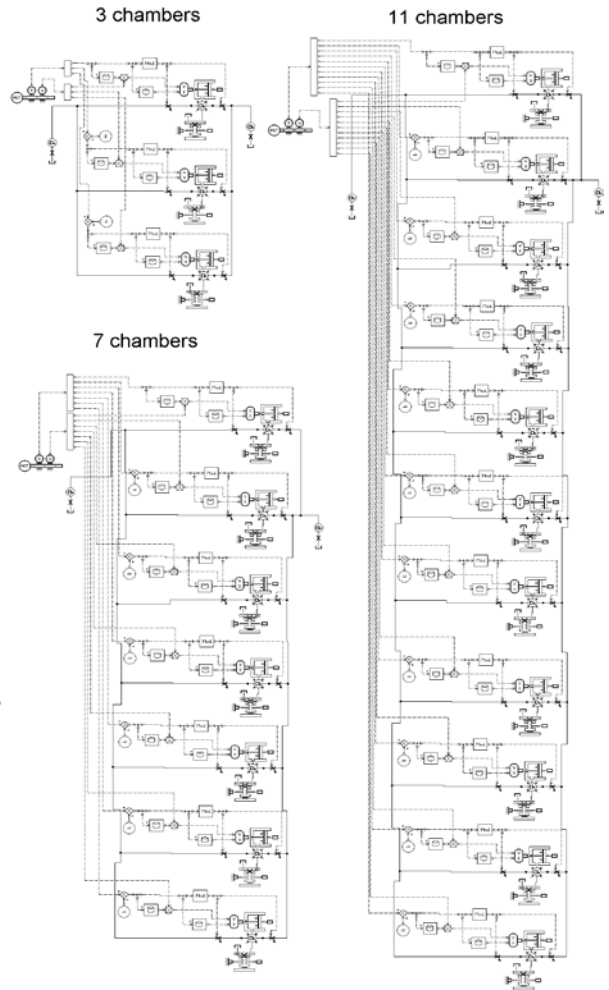


Fig. 29: Generic pump models with scalar elements

Geometric features of the virtual unit are inputs to the hydraulic submodels through data files at A and B on which cubic spline interpolations occur (*general geometric submodels*). Submodel A manages chamber volumes and their derivatives, submodel B the flow passage areas with inlet and delivery volumes. In this layout submodel F accounts for constant geometry leakage paths between chambers and oil sump.

Conversely, Fig. 29 details models of that same unit built through standard submodels for the cases of 3, 7 and 11 chambers. It can be easily argued that, with this approach, changing the number of chambers is not a painless task. Geometry is provided in exactly the same way i.e. through the aforementioned data files used in Fig. 28 and attained results are, in all instances, obviously equal. A comparison of CPU time for the two approaches is detailed in Fig. 30: simulations have been performed on a Sun-Blade-1000 (UltraSPARC III 750 MHz, and 512 MB RAM) over a time frame of 0.06 seconds (three shaft revolutions @3000 rpm) with a communication interval of 10^{-5} seconds and a tolerance of 10^{-5} .

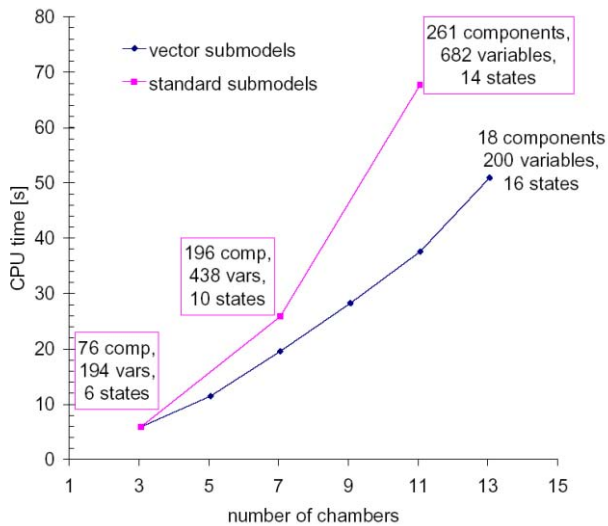


Fig. 30: CPU time vs number of chambers for vector and scalar submodels

It can be recognized that with vector submodels an increase in the number of chambers is less influential than for the scalar approach; this is consequent to the fact that using standard submodels, their number and associated variables increase with the number of chambers, whereas with vector submodels these remain constant since the layout stands invariable.

The number of states in the vector model is constant and equal to $N_{\max}+3$ (13 chambers pressures, pressures in the inlet and delivery ambients and shaft angular position) whereas the scalar model involves $N+3$ states. On a factual basis, this does not turn out to be an advantage as far as CPU time is concerned. An additional and significant point in bias of the vector model of Fig. 28 stays in the fact that it also and readily allows the determination of instantaneous torque (with the component A) and ideal flow ripple (component C). Attainment of these information through standard submodels in Fig. 29 involves additional interventions and complexities.

9 Appendix B

The suction pipe and inlet duct of a lube pump can be modelled taking advantage of the Hydraulic Resistance Library (Fig. 14). Two differences exist with the Standard Hydraulic Library. In the first place hydraulic resistance submodels make use of *total* rather than *static* pressure. This is most appropriate in the specific case where the influence of kinetic energy variations is dominant in the evaluation of flow resistance. In the second place loss coefficients are already accounted within submodels once geometry is assigned. On the contrary, use of orifices in the Standard Library requires knowledge of flow coefficients to be determined by experiments. The pump suction subsystem is shown in Fig. 31 along with the hydraulic scheme and the model based on the Hydraulic Resistance Library.

For this subsystem and at pump inlet (approx. point 5 in Fig. 31), simulated pressure values vs flow rate,

are collected in Fig. 32. At that same location, fluid velocity, at max flow, is not particularly high (about 4m/s), however dynamic pressure, though small in absolute terms (0.07 bar) still amounts to 25% of total pressure.

A simulation of this same case performed with the Standard Library (total and static pressure coincide) would have introduced a non negligible approximation.

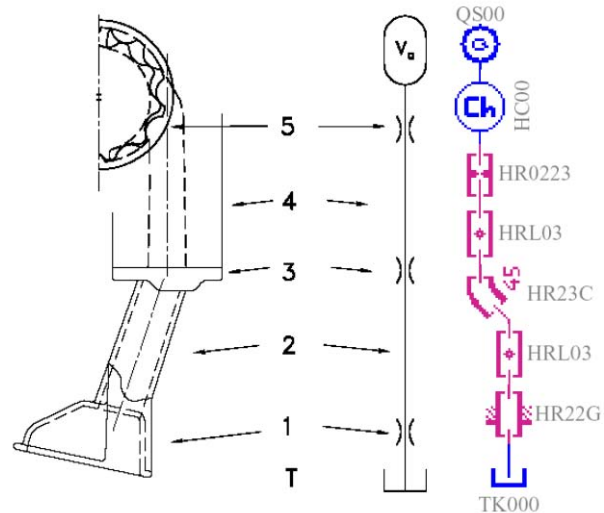


Fig. 31: Pump suction subsystem, its hydraulic scheme and modelling through the Hydraulic Resistance Library

10 Conclusions

This paper has considered the significant role that simulation has on the design process of hydraulic lube pumps and has put forward basic vector elements such as variable volumes, flow areas, nodes and hydraulic vector lines that lead to a unified simulation approach of volumetric pumps. It has also stressed the need of testing to establish that incomplete chamber filling is the main cause for observed discrepancies.

Problems regarding recirculation of excess flow and airborne noise, though cited, have not been addressed since they form topics of detailed research work, done by the same authors, documented elsewhere (see References).

11 Some Technical Details

The system presented in Fig. 14 consists of 34 state variables and two implicits. On a Sun Ultra 10 Workstation (UltraSPARC-IIi 300 MHz with 192 Mb RAM), the time required to simulate a complete shaft revolution at 3000 rpm is about 1.5 minutes with a communication interval of 10^{-5} s and a tolerance of 10^{-5} . Attainment of a flow-pressure steady state characteristic re-

quires from 5 to 10 minutes.

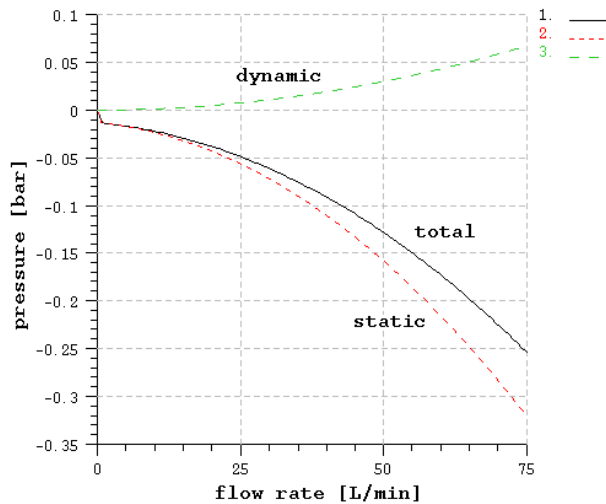


Fig. 32: Dynamic, total and static pressure at pump inlet A passage area

Nomenclature

A	passage area
N	number of chambers
p	pressure
Q	flow rate
t	time
V	chamber volume
β	bulk modulus
φ	angular position
ω	angular speed

Subscripts

a	inflow
j	j-th chamber
m	outflow

References

- Mancò, S., Nervegna, N., Rundo, M. et al. 1998. Gerotor Lubricating Oil Pump for IC Engines, *SAE paper 982689 and SAE Transactions (Journal of Engines)*.
- Fabiani, M., Mancò, S., Nervegna, N., Rundo, M. et al. 1999. Modelling and Simulation of Gerotor Gearing in Lubricating Oil Pump. *SAE Paper 1999-01-0626 and SAE Transactions (Journal of Engines)*.
- Mancò, S., Nervegna, N., Rundo, M. 1999. Influenza della velocità di rotazione sul comportamento delle pompe di lubrificazione dei motori a combustione interna. *54 Congresso Nazionale ATI, 14-17 Settembre, L'Aquila*.
- Mancò, G., Mancò, S., Rundo, M., Nervegna, N. 2000. Computerized generation of novel gearings

for internal combustion engines lubricating pumps, *International Journal of Fluid Power*, Vol. 1, No. 1, ISSN 1439-9776.

Mancò, S., Nervegna, N., Rundo, M. 2000. Effects of timing and odd/even number of teeth on noise generation of gerotor lubricating pumps for IC Engines, *SAE paper 2000-01-2630, also in SAE Special Publication, Topics in Hydraulics (SP-1554) ISBN 0-7680-0649-X; 2000 SAE International Off-Highway & Powerplant Congress and Exposition, Milwaukee WI, USA September 11-13, 2000. SAE Transactions (Journal of Commercial Vehicles)*.

Mancò, S., Nervegna, N., Rundo, M. 2000. Studio sulla pompa a portata variabile. *Unpublished progress report to Pierburg SpA. AMESim Manual Version 3.5, 2001, IMAGINE, Roanne*.

Mancò, S., Nervegna, N., Rundo, M. 2001. Critical Issues on Performance of Lubricating Gerotor Pumps at High Rotational Speed. *The Seventh Scandinavian International Conference on Fluid Power. SICFP'01, Lynköping, Sweden, May 30-June 1, Vol.2, pp. 23-37*.

Mancò, S., Nervegna, N., Rundo, M. 2001. Variable flow internal gear pump. *Proceedings of the 2001 ASME International Mechanical Engineering Congress and Exposition, Nov. 11-16, New York, NY. IMECE2001/FPST-2*.



Salvatore Mancò

Graduated in Mechanical Engineering (1980) from Politecnico di Torino, Italy. His scientific career started on diesel fuels quality, SI engine supercharging and control, and landed, in the 2nd half of the eighties, on fluid power. S. Mancò main contribution to the Fluid Power Scientific community is on the gear pump field. Since 1992, he is associate professor of Energy Systems at Politecnico di Torino.



Nicola Nervegna

Graduate in Nuclear Engineering (1971) from Politecnico di Torino, Italy. He joined the Politecnico staff in October 1971 and, at present, is Professor of Fluid Power Systems. His research interests lie in the broad fields of Fluid Power with involvement in positive displacement pumps as well in the modelling, simulation and testing of various hydraulic components.



Massimo Rundo

Graduated in Mechanical Engineering (1996) from Politecnico di Torino. After graduation he participated within the Fluid Power Group of the Politecnico di Torino, as a Magneti Marelli visiting researcher, to an extensive and ongoing research project on gerotor and external gear pumps for internal combustion engines lubrication. He is very active in modelling, simulation and testing of fluid power components.